Quantum phase transition using quantum walks in an optical lattice

C. M. Chandrashekar[1] and Raymond Laflamme[1,2]
[1]*Institute for Quantum Computing, University of Waterloo, Waterloo, Ontario, Canada N2L 3G1*
[2]*Perimeter Institute for Theoretical Physics, Waterloo, Ontario, Canada N2J 2W9*
(Received 13 September 2007; revised manuscript received 12 May 2008; published 11 August 2008)

We present an approach using quantum walks (QWs) to redistribute ultracold atoms in an optical lattice. Different density profiles of atoms can be obtained by exploiting the controllable properties of QWs, such as the variance and the probability distribution in position space using quantum coin parameters and engineered noise. The QW evolves the density profile of atoms in a superposition of position space, resulting in a quadratic speedup of the process of quantum phase transition. We also discuss implementation in presently available setups of ultracold atoms in optical lattices.

DOI: 10.1103/PhysRevA.78.022314 PACS number(s): 03.67.Lx, 03.65.−w, 03.75.Lm, 05.30.Jp

I. INTRODUCTION

Exploiting aspects of quantum mechanics, such as superposition and interference, has led to the idea of quantum walks (QWs), a generalization of classical random walks (CRWs) [1–5]. In the CRW the particle moves in the configuration space with a certain probability, whereas in the QW the particle moves in a superposition of the configuration space with a probability amplitude. Because of the quantum interference effect, the variance in position σ^2 of the QW is known to grow quadratically with the number of steps N, $\sigma^2 \propto N^2$, compared to the linear growth, $\sigma^2 \propto N$, for the CRW. This motivated research in the direction of finding quantum algorithms with optimal efficiency using the QW [6–9]. Experimental implementation of the QW has also been reported [10–12].

The continuous time quantum walk (CTQW) and the discrete time quantum walk (DTQW) are two widely studied versions of the QW [13]. In the CTQW [14], one can directly define the walk on the position space, whereas, in the DTQW [15] it is necessary to introduce a quantum coin operation to define the direction in which the particle has to move. Due to the coin degree of freedom, the discrete time variant is shown to be more powerful than the other in some contexts [9], and the coin parameters (scattering operator) can be varied to control the dynamics of the evolution [4,16]. Therefore, in this paper we will consider only the discrete time variant of the QW. Beyond quantum computation, the QW can be used to demonstrate coherent quantum control over, for example, atoms, photons, or spin chain systems. Along with purely quantum dynamics, a small amount of engineered noise or environmental effect can enhance the properties of the QW [17–19]. As we show later this can enlarge the toolbox for controlling the dynamics in a physical system.

This paper describes the use of a QW which consists of an iteration of the quantum coin operation and a subsequent conditional shift operation to control and study the dynamics of ultracold bosonic atoms in an optical lattice. The quantum coin operation evolves the atom wave function into a superposition of the internal state of the particle and the shift operation spreads the atom wave function in a superposition of the position space. In particular, we show that the quantum phase transition from the Mott insulator (MI)—a regime where no phase coherence is prevalent—to the superfluid (SF)—a regime with long-range phase coherence [20,21]—and vice versa can be obtained by redistributing the density profile of atoms using a QW. The simulation of the quantum phase transition using the QW occurs quadratically faster in one dimension (1D) compared to, varying the optical lattice depth and letting the atom-atom interaction follow the CRW behavior. Enhancing the properties of the QW by varying the quantum coin parameters or by addition of experimentally engineered noise in small amounts [18] can be used as an additional tool to evolve the atoms into different number density distributions.

Theoretical studies of the dynamics of atoms in an optical lattice are done using mean field approaches [22] and quantum Monte Carlo methods [23]. The quantum correlation induced between atoms and position space by the QW can serve as an alternate method for theoretical studies. The use of the QW to study the dynamics of particles in 1D magnetic systems [24], and photonic Mott insulators [25] or to observe complex quantum phase transitions [26] and quantum annealing [27] would be of both theoretical and experimental relevance.

This paper is organized as follows. In Sec. II we define the DTQW and its properties, and in Sec. III the phase transition in an optical lattice is discussed. The implementation of the QW on atoms in 1D MI and SF regimes is discussed in Sec. IV, where we analyze the dynamics and present the density profile obtained by exploiting some of the properties of the QW. In Sec. V we discuss the QW with a noisy channel as a tool to control the redistribution of atoms. In Sec. VI we briefly discuss a scheme for experimental realization before concluding in Sec. VII.

II. DISCRETE TIME QUANTUM WALK

To define a 1D DTQW we require the *coin* Hilbert space $\mathcal{H}_c$ and the *position* Hilbert space $\mathcal{H}_p$. $\mathcal{H}_c$ is spanned by the internal state of the particle, $|0\rangle$ and $|1\rangle$, and $\mathcal{H}_p$ is spanned by the basis states $|j\rangle$, $j \in \mathbb{Z}$. The total system is then in the space $\mathcal{H}=\mathcal{H}_c \otimes \mathcal{H}_p$. To implement the QW, the particle at the origin ($j=0$) in state $|j_0\rangle$ is evolved into a superposition of $\mathcal{H}_c$,

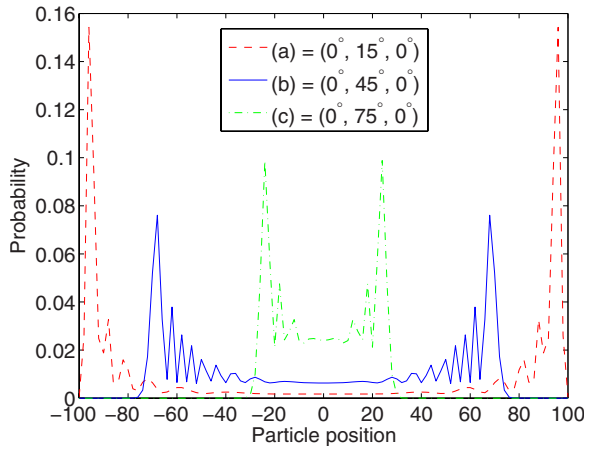

FIG. 1. (Color online) Spread of probability distribution for different values of θ using the quantum coin operator $B_{0,\theta,0}$. The distribution is wider for (a) $(0,\pi/12,0)$ than for (b) $(0,\pi/4,0)$ and (c) $(0,5\pi/12,0)$, showing the decrease in spread with increase in θ. The initial state of the particle $|\Psi_{\text{in}}\rangle=(|0\rangle+i|1\rangle)\otimes|j_0\rangle$ and the distribution is for 100 steps.

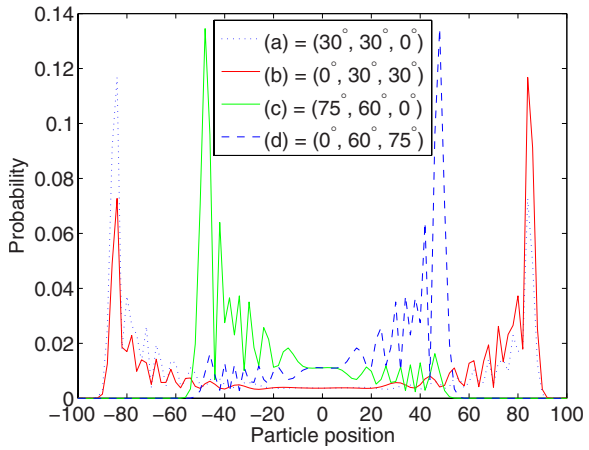

FIG. 2. (Color online) Spread of probability distribution for different values of ξ,θ,ζ using quantum coin operator $B_{\xi,\theta,\zeta}$. Biasing the walk using ξ shifts the distribution to the left: (a) $(\pi/6,\pi/6,0)$ and (c) $(5\pi/12,\pi/3,0)$. Biasing the walk using ζ shifts it to the right: (b) $(0,\pi/6,\pi/6)$ and (d) $(0,\pi/3,5\pi/12)$. The initial state of the particle $|\Psi_{\text{in}}\rangle=(|0\rangle+i|1\rangle)\otimes|j_0\rangle$ and the distribution is for 100 steps.

$$|\Psi_{\text{in}}\rangle=\frac{1}{\sqrt{2}}[|0\rangle+i|1\rangle]\otimes|j_0\rangle \tag{1}$$

and then subjected to the conditional shift operation S to evolve into a superposition in the position space:

$$S=|0\rangle\langle 0|\otimes\sum_{j\in\mathbb{Z}}|j-1\rangle\langle j|+|1\rangle\langle 1|\otimes\sum_{j\in\mathbb{Z}}|j+1\rangle\langle j|$$
$$\equiv|0\rangle\langle 0|\otimes\hat{a}+|1\rangle\langle 1|\otimes\hat{a}^{\dagger}. \tag{2}$$

Here $\hat{a}$ and $\hat{a}^{\dagger}$ are annihilation and creation operations acting on $\mathcal{H}_p$. The S is followed by the quantum coin operation, which in general can be written as an SU (2) operator of the form

$$B_{\xi,\theta,\zeta}=\begin{pmatrix} e^{i\xi}\cos(\theta) & e^{i\zeta}\sin(\theta) \\ e^{-i\zeta}\sin(\theta) & -e^{-i\xi}\cos(\theta)\end{pmatrix}, \tag{3}$$

to evolve the particle into a superposition in $\mathcal{H}_c$. Therefore, each step of the QW is composed of an application of operation B and a subsequent operation S to entangle $\mathcal{H}_c$ and $\mathcal{H}_p$. The process of application of $W=S(B_{\xi,\theta,\zeta}\otimes\mathbb{1})$ is iterated without resorting to intermediate measurements to realize a large number of steps.

The variance can be varied by changing the parameter θ,

$$\sigma^2\approx[1-\sin(\theta)]N^2. \tag{4}$$

The effect of the parameter θ on the distribution is shown in Fig. 1; the variance decreases with increase in the value of θ. The parameters ξ and ζ introduce asymmetry in the position space probability distribution as shown in Fig. 2 and their effect on the variance is negligible [16]. The simplest coin operation is the Hadamard operator $H=B_{0,45°,0}$. In this paper, Sec. IV, we consider a QW with $B_{0,\theta°,0}$ to redistribute atoms in an optical lattice. The QW is sensitive to noise [17–19] but in Sec. V we consider small amounts of three physically relevant models of noise that can be experimentally induced: a bit-flip channel, a phase-flip channel, and an amplitude-damping channel [18], to act as an enhanced toolbox to control the dynamics of the atoms.

III. PHASE TRANSITION IN OPTICAL LATTICE

A Bose-Einstein condensate (BEC) at low enough temperature is a SF described by a wave function that exhibits long-range coherence [28]. When the BEC is transferred to the lattice potential, the atoms move from one lattice site to the next by tunnel coupling. Using a second-quantized form, the system can be described by the Bose-Hubbard model:

$$H=-J\sum_{\langle j,k\rangle}\hat{b}_j^{\dagger}\hat{b}_k+\sum_j\epsilon_j\hat{n}_j+\frac{1}{2}U\sum_j\hat{n}_j(\hat{n}_j-1), \tag{5}$$

J is the tunneling term characterized by the hopping amplitude, $\hat{b}_j$ and $\hat{b}_j^{\dagger}$ are the annihilation and creation operators of atoms, ϵ_j denotes the energy offset due to external harmonic confinement of the atoms in the jth lattice site, $\hat{n}_j=\hat{b}_j^{\dagger}\hat{b}_j$ is the atomic number operator counting the number of atoms, and U is the repulsive interaction between two atoms in a single lattice site.

When J dominates the Hamiltonian, the ground-state energy is minimized if the single-particle wave functions of all N atoms are spread out over the entire M-lattice site. If ϵ_j =const (homogeneous system) then the many-body ground state is called the SF state and is given by

$$|\psi_{\text{SF}}\rangle_{U=0}\propto\left(\sum_{j=1}^{M}\hat{b}_j^{\dagger}\right)^N|V\rangle, \tag{6}$$

where $|V\rangle$ is a vacuum state. In this state the probability distribution for the local occupation n_j of atoms on a single lattice site is Poissonian. The state is well described by a macroscopic wave function with long-range phase coherence

throughout the lattice. With increase in the ratio U/J, the system reaches a quantum critical point, the fluctuations in atom number of a Poisson distribution become energetically very costly, and the ground state of the system will instead undergo a quantum phase transition from the SF state to the MI state, a product of local Fock states of n atoms in each lattice site given by [20,21],

$$|\psi_{\mathrm{MI}}\rangle_{J=0} \propto \prod_{j=1}^{M} (\hat{b}_j^{\dagger})^n |V\rangle. \tag{7}$$

IV. QUANTUM WALK ON ATOMS IN 1D MOTT INSULATOR REGIME

Localized atomic wave functions in the MI regime with one atom in each of the M lattice sites are initialized into a symmetric superposition of any of the two internal trappable-state, hyperfine levels $|0\rangle$ and $|1\rangle$ [29],

$$|\Psi_{\mathrm{MI}}\rangle_{J=0} \propto \prod_{j=-M/2}^{M/2} \left(\frac{|0\rangle + i|1\rangle}{\sqrt{2}} \right) \otimes |j\rangle. \tag{8}$$

The $\mathcal{H}_c$ of each atom is spanned by the two hyperfine levels and $\mathcal{H}_p$ is spanned by the lattice site. The total system is then in the Hilbert space $\mathcal{H}_m = (\Pi_j \mathcal{H}_{c_j}) \otimes \mathcal{H}_p$. The unitary shift operation S, Eq. (2), on the above system will evolve each atom into a superposition of the neighbor lattice site, establishing the quantum correlation between the states of the atom and the neighboring lattice site,

$$S|\Psi_{\mathrm{MI}}\rangle_{J=0} \propto \prod_{j=-M/2}^{M/2} \left(\frac{|0\rangle \otimes \hat{a}|j\rangle + i|1\rangle \otimes \hat{a}^{\dagger}|j\rangle}{\sqrt{2}} \right). \tag{9}$$

To implement the N number of steps, the process of $W = S(B_{\xi,\theta,\zeta} \otimes \mathbb{1})$ is iterated N times. During the iteration, the atoms and position correlations interfere resulting in,

$$(W)^N |\Psi_{\mathrm{MI}}\rangle_{J=0} \propto \prod_{j=-M/2}^{M/2} (\beta_{j-N}|0\rangle \otimes |j-N\rangle + \beta_{j-(N+1)}|0\rangle \otimes |j-(N+1)\rangle + \cdots + \beta_{j+N}|0\rangle \otimes |j+N\rangle + \gamma_{j-N}|1\rangle \otimes |j-N\rangle + \cdots + \gamma_{j+N}|1\rangle \otimes |j+N\rangle). \tag{10}$$

This can be written as

$$(W)^N |\Psi_{\mathrm{MI}}\rangle_{J=0} \propto \prod_{j=-M/2}^{M/2} \left(\sum_{x=j-N}^{j+N} [\beta_x|0\rangle + \gamma_x|1\rangle] \otimes |x\rangle \right); \tag{11}$$

β_x and γ_x are the probability amplitudes of states $|0\rangle$ and $|1\rangle$ at lattice site x, which range from $(j-N)$ to $(j+N)$. For a QW of N steps on a particle initially at position $j=0$ using $B_{0,\theta,0}$ as the quantum coin, the probability distribution spreads over the interval $(-N\cos(\theta), N\cos(\theta))$ in position space and shrinks quickly outside this region [16,30]. Therefore, after N steps the density profile of M atoms initially between $\pm M/2$ will correlate with the position space and spread over the lattice site $\pm[M/2 + N\cos(\theta)]$. Figure 3 is the redistribution of atomic density of 40 atoms initially in the MI state when subjected to a QW of different numbers of steps with Hadamard operator $H = B_{0,45^\circ,0}$ as the quantum coin.

The redistributed atoms would be in either of their internal states and this can be retained to study the phase transition of two-state bosonic atoms in an optical lattice [31] or all atoms can be transferred to one of the internal states. A technique based on adiabatic passage using crafted laser pulses can be used for a nearly complete transfer of population between two states [32], and a popular example of one such technique is stimulated Raman adiabatic passage (STIRAP) [33].

Along with the correlation between the atoms and the position space, Eq. (10) also reveals the overlap of the probability amplitude of different atoms in the position space. That is, during each step of the QW, the amplitude of the states of each atom overlaps with the amplitude of the states of the atoms in the neighboring lattice site. After the iteration of the N steps $\geqslant M/2/\cos(\theta)$, the overlap of all atoms could be seen at the central region of the lattice. But $M/2/\cos(\theta)$ number of steps is not sufficient for all M atoms to also be in

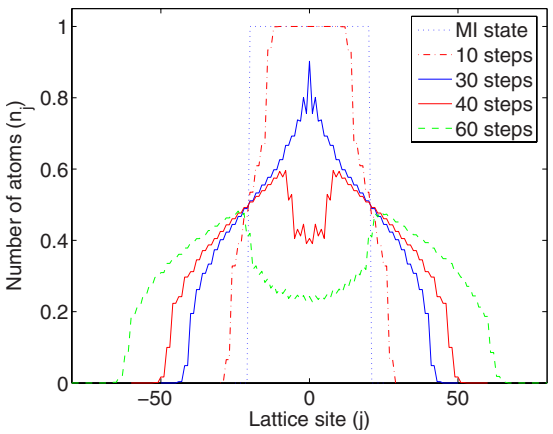

FIG. 3. (Color online) Density profile of the evolution of 40 atoms starting from MI state in correlation with the position space when subjected to a QW of different numbers of steps with the Hadamard operator $B_{0,45^\circ,0}$ as the quantum coin. The distribution spreads with increase in the number of steps.

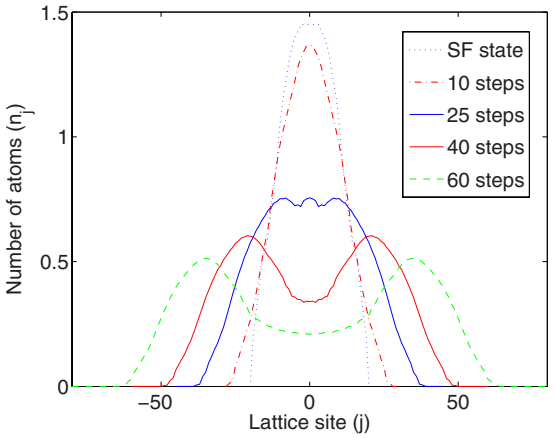

FIG. 4. (Color online) Density profile of the evolution of 40 atoms starting from SF state in correlation with the position space when subjected to a QW of different numbers of steps with the Hadamard operator $B_{0,45°,0}$ as the quantum coin. The distribution spreads with increase in the number of steps and is almost uniform between the lattice sites ± 20 when $N=25$. At this stage the optical potential depth can be increased to cancel the correlation and obtain the MI state.

correlation with the entire M-lattice site and this is one of the requirements to observe the SF state. When the atoms are in correlation with the entire lattice site, then they are also in correlation with all other atoms and hence, in this paper, we discuss the evolution in terms of correlation between atoms and position space.

When the number of steps of the QW is equal to the number of lattice sites ($N=M$), the overlap of a fraction of the amplitude of all M atoms exist within the lattice site $\pm M\cos(\theta)/2$, making the region identical to the SF state. Beyond $\pm M\cos(\theta)/2$ the number of atoms in correlation with that position space decreases and hence the number of ovrlapping atoms also decrease. To make all M atoms spread between lattice sites $\pm M/2$ using the usual method of lowering the optical potential depth following the CRW protocol takes M^2 steps. Therefore, we can conclude that using the QW a long-range correlation can be induced quadratically faster than by the usual technique.

Similarly, Fig. 4 is the redistribution of atomic density of 40 atoms initially in the SF states when subjected to QWs of different numbers of steps using the Hadamard operator $B_{0,45°,0}$ as the quantum coin. To reach the MI state the distribution should be uniform over the lattice sites without correlation. A distribution that is approximately uniform within the region $\pm M/2$ can be obtained using the QW. In Fig. 4, when $N=25$ the distribution is almost uniform between the lattice sites ± 20, retaining the correlation with the position space. The uniformity of the distribution can be improved by using the tunneling of atoms between the lattice. Once the distribution is uniform, the optical potential depth can be increased to cancel the correlation and obtain the MI state. The uniformity of the distribution can also be improved by introducing a noise channel, as we show later.

The variance and the probability distribution can be controlled using the parameters θ, ξ, and ζ in $B_{\xi,\theta,\zeta}$. Figures 5 and 6 shows the density distribution obtained by implementing the QW on atoms in MI and SF states ($N=M=40$) with different values of θ in the coin operator $B_{0,\theta,0}$. The spread is wider for $\theta=30°$ and decreases with increase in θ. In Fig. 6 the distribution is almost uniform for $\theta=60°$ between the lattice sites ± 20. At this value the optical potential depth can be increased to cancel the correlation and obtain the MI state.

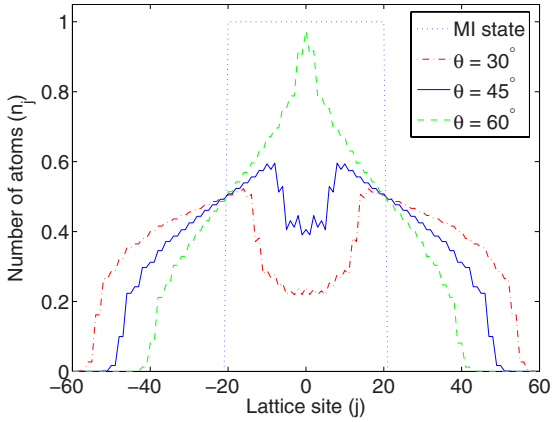

FIG. 5. (Color online) Distribution of atoms initially in MI state when subjected to a QW ($N=M=40$) using different values for θ in the coin operator $B_{0,\theta,0}$. The spread is wider for $\theta=30°$ and decreases with increasing θ.

The Hamiltonian of the system in general can be described by the 1D Bose-Hubbard model for two-state atoms,

$$H = -J_{\uparrow}\sum_{\langle j,k\rangle}\hat{b}^{\dagger}_{j\uparrow}\hat{b}_{k\uparrow} - J_{\downarrow}\sum_{\langle j,k\rangle}\hat{b}^{\dagger}_{j\downarrow}\hat{b}_{k\downarrow} + \sum_{j,\alpha=\uparrow,\downarrow}\epsilon_{j,\alpha}\hat{n}_{j,\alpha} + U\sum_{j}\left(\hat{n}_{j\uparrow}-\frac{1}{2}\right)\left(\hat{n}_{j\downarrow}-\frac{1}{2}\right) + \frac{1}{2}\sum_{j,\alpha=\uparrow,\downarrow}V_{\alpha}\hat{n}_{j\alpha}(\hat{n}_{j\alpha}-1) + \sum_{j}(d_L\hat{b}^{\dagger}_{(j-1)\uparrow}\hat{b}_{j\uparrow} + d_R\hat{b}^{\dagger}_{(j+1)\downarrow}\hat{b}_{j\downarrow}), \quad (12)$$

Here $\uparrow$ and $\downarrow$ represent the terms for atoms in state $|0\rangle$ and

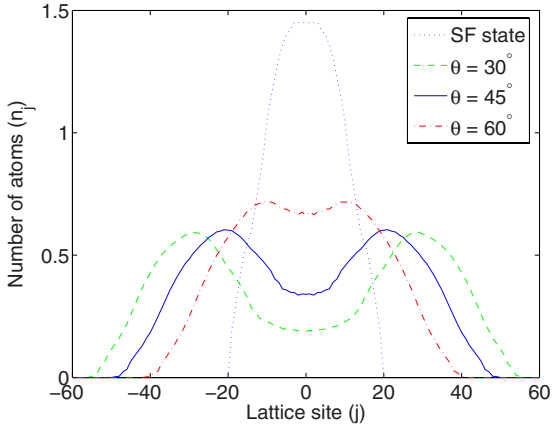

FIG. 6. (Color online) Distribution of atoms initially in SF state when subjected to a QW ($N=M=40$) using different values for θ in the coin operator $B_{0,\theta,0}$. The distribution is almost uniform for $\theta=60°$ between the lattice sites ± 20. At this value the optical potential depth can be increased to cancel the correlation and obtain the MI state.

state $|1\rangle$, respectively. U is the interaction between atoms in states $|0\rangle$ and $|1\rangle$; $V_{\uparrow(\downarrow)}$ is the interaction between atoms in the same state. d_L and d_R are the left and right displacement terms induced during each step of the QW. The Hamiltonian is evolved using a coin toss operation in a regular interval of time t, the time required to move the atom to the neighboring site. The optical lattice can be dynamically manipulated to evolve atoms in a superposition of lattice sites without giving time for the atom-atom interaction, and the optical potential depth of the system can be configured just above the level where there is no direct tunneling. Then the dynamics of atoms in lattice will be dominated by the last term of the Hamiltonian in Eq. (12) ignoring the atom-atom interaction. Therefore scaling up the scheme of using the QW to systems with large numbers of atoms in each lattice site or to infinitely large numbers of lattice site is also straightforward; whereas the atom-atom interaction plays a prominent role during the usual method of varying the potential depth.

V. QUANTUM WALK WITH A NOISY CHANNEL AS A TOOLBOX

Along with the coin parameters θ, ξ, and ζ, a small amount of engineered noise can be used to control the redistribution of atoms in the optical lattice. To demonstrate the effect of the QW with a noisy channel on atoms in an optical lattice we consider a bit-flip channel, a phase-flip channel, and an amplitude-damping channel. The bit-flip channel flips the state of the particle from $|0\rangle$ ($|1\rangle$) to $|1\rangle$ ($|0\rangle$) (Pauli X operation) and a phase-flip channel flips the phase of $|1\rangle$ to $-|1\rangle$ (Pauli Z operation). We use the notation p for the noise level where $0 \leqslant p \leqslant 1$. Therefore, the bit- (phase-)flip channel flips the state (phase) with probability $(1-p)$ during each step of the QW. An amplitude-damping channel leaves state $|0\rangle$ unchanged but reduces the amplitude of state $|1\rangle$ with probability $(1-p)$ resulting in an asymmetric distribution. The maximum decoherence effect using bit- and phase-flip channels is at $p=0.5$ due to symmetries induced by these two channels during the QW; whereas the amplitude-damping channel does not obey any symmetry and hence the maximum effect is for $p=1$ [18]. Our numerical implementation of these channels evolves the density matrix employing the Kraus operator representation.

Figure 7 is a comparison of the distribution obtained without noise channels to the distributions with phase-flip ($p=0.02$ and $p=0.1$) and amplitude-damping channels ($p=0.2$) on atoms initially in the MI state. Similarly, the redistribution of atoms in the SF state when subjected to a QW without and with noise channels is shown in Fig. 8. With the addition of phase-flip noise of $p=0.02$, a uniform distribution is obtained. Then the optical potential depth can be increased to cancel the correlation and obtain the MI state.

The effect of bit-flip on the distribution is close to the one obtained using the phase-flip channel and hence the redistribution in Figs. 7 and 8 are shown only for phase-flip and amplitude-damping channels. Increasing noise level affects the variance of the QW [18], which proportionally affect the atom-position correlation and the atom-atom overlap. Therefore it is important to restrict the noise level to a very low value ($p \lessapprox 0.1$) to use the noisy channel as a tool.

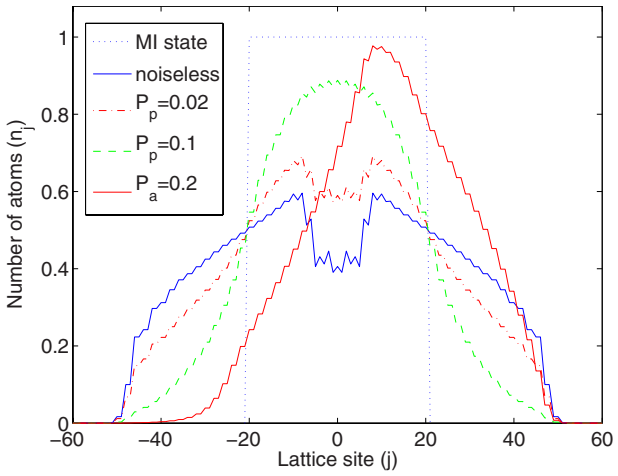

FIG. 7. (Color online) Atoms in MI state after implementing the QW ($N=M=40$, $\theta=45°$) with noise channel. With increased phase damping from $p_p=0.02$ to 0.1 the distribution (n_j) at the central region gets closer to Gaussian. Amplitude damping of the state $|1\rangle$ introduces asymmetry to the distribution; $p_a=0.2$.

Some of the distribution presented in Secs. IV and V using QWs look similar to some of the distributions presented using different techniques; in [34] using time evolution density matrix renormalization group and in [35,36] using quantum Monte Carlo simulation. These techniques present the change in density profile distribution with time, whereas in this paper we have discussed the change with number of steps of the QW.

VI. IMPLEMENTATION

Optical lattices ranging from simple periodic, square, and cubic to a more exotic ones, such as hexagonal and Kagome

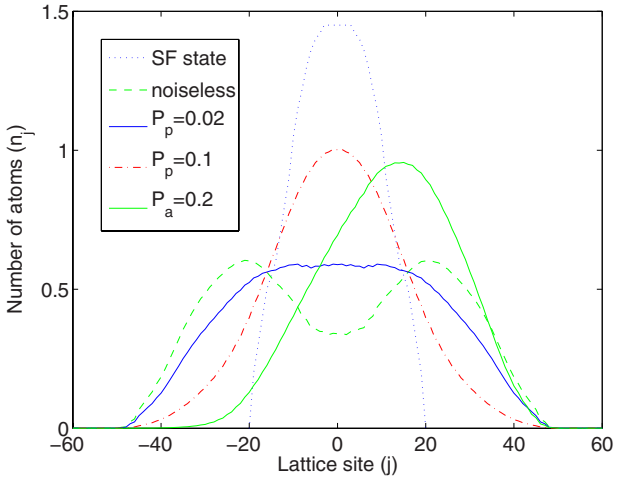

FIG. 8. (Color online) Atoms in SF state after implementing a QW ($N=M=40$, $\theta=45°$). With a noiseless QW, the atoms spread, getting close to a uniform distribution. For phase damping $p_p=0.02$ the distribution is uniform between ± 20 and gets closer to Gaussian at $p_p=0.1$. Amplitude damping of the state $|1\rangle$ introduces asymmetry to the distribution, $p_a=0.2$.

lattices using the superlattice technique [37] have been created to trap and manipulate cold atoms. Manipulation of cold atoms in a time-varying optical lattice has also been reported [38]. This has provided flexibility in designing and studying quantum phases and quantum phase transitions in coherent and strongly correlated ultracold atoms.

In Ref. [39], controlled coherent transportation of rubidium atoms in the spin-dependent optical lattice has been experimentally demonstrated. Rubidium atoms in the MI state are evolved into superposition of two internal states and the two states are transported in opposite directions. Delocalization of atoms over seven lattice sites is demonstrated. This scheme can be adopted to implement the QW and to redistribute the density profile by introducing a rf pulse [29] after each separation. An additional rf pulse can be engineered to act as noise channels.

In an implementation scheme proposed in Ref. [40], a *stimulated Raman kick*, two selected levels of the atom are coupled to the two modes of counterpropagating laser beams to impart a translation of atoms in the position space. To realize the transition from the SF to the MI phase using this scheme, atoms are first redistributed by implementing the QW in a long-Rayleigh-range optical trap [41] and the optical lattice is switched on at the end to confine atoms and cancel the correlation. For the transition from MI to SF, the atoms initially in the optical lattice are transferred to a long-Rayleigh-range dipole trap and a QW is implemented.

VII. CONCLUSION

In this paper, we have shown the use of the QW to study the dynamics of atoms in an optical lattice and expedite the process of quantum phase transition. We have also used the QW with experimentally realizable noisy channels to show the additional control one can have over the evolution and atomic density redistribution. Theoretically, the evolution of the density profile with a QW can be used in place of quantum Monte Carlo simulation to study the correlation and redistribution of atoms in optical lattices. We expect the QW to play a wider role in simulating and expediting the dynamics in various physical systems.

ACKNOWLEDGMENTS

We thank Gerardo Ortiz for helpful discussion. This work was funded by CIFAR, ARO, and MITACS. C.M.C. would like to thank Mike and Ophelia Lezaridis for financial support at IQC.

[1] G. V. Riazanov, Sov. Phys. JETP **6**, 1107 (1958).
[2] R. P. Feynman and A. R. Hibbs, *Quantum Mechanics and Path Integrals* (McGraw-Hill, New York, 1965).
[3] Y. Aharonov, L. Davidovich, and N. Zagury, Phys. Rev. A **48**, 1687 (1993).
[4] David A. Meyer, J. Stat. Phys. **85**, 551 (1996).
[5] David A. Meyer, Phys. Rev. E **55**, 5261 (1997); J. Phys. A **34**, 6981 (2001).
[6] A. M. Childs, R. Cleve, E. Deotto, E. Farhi, S. Gutmann, and D. A. Spielman, in *Proceedings of the 35th ACM Symposium on the Theory of Computing* (ACM Press, New York, 2003), p. 59.
[7] N. Shenvi, J. Kempe, and K. Birgitta Whaley, Phys. Rev. A **67**, 052307 (2003).
[8] A. M. Childs and J. Goldstone, Phys. Rev. A **70**, 022314 (2004).
[9] A. Ambainis, J. Kempe, and A. Rivosh, in *Proceedings of ACM-SIAM Symposium on Discrete Algorithms (SODA) 2005* (ACM, New York, 2005), pp. 1099–1108.
[10] C. A. Ryan, M. Laforest, J. C. Boileau, and R. Laflamme, Phys. Rev. A **72**, 062317 (2005).
[11] J. Du, H. Li, X. Xu, M. Shi, J. Wu, X. Zhou, and R. Han, Phys. Rev. A **67**, 042316 (2003).
[12] H. B. Perets, Y. Lahini, F. Pozzi, M. Sorel, R. Morandotti, and Y. Silberberg, Phys. Rev. Lett. **100**, 170506 (2008).
[13] Julia Kempe, Contemp. Phys. **44**, 307 (2003).
[14] E. Farhi and S. Gutmann, Phys. Rev. A **58**, 915 (1998).
[15] A. Ambainis, E. Bach, A. Nayak, A. Vishwanath, and J. Watrous, in *Proceedings of the 33rd Symposium on the Theory of Computing* (ACM, New York, 2001), pp. 60–69.
[16] C. M. Chandrashekar, R. Srikanth, and R. Laflamme, Phys. Rev. A **77**, 032326 (2008).
[17] V. Kendon and B. Tregenna, Phys. Rev. A **67**, 042315 (2003).
[18] C. M. Chandrashekar, R. Srikanth, and S. Banerjee, Phys. Rev. A **76**, 022316 (2007).
[19] Todd A. Brun, Hilary A. Carteret, and A. Ambainis, Phys. Rev. Lett. **91**, 130602 (2003).
[20] D. Jaksch, C. Bruder, J. I. Cirac, C. W. Gardiner, and P. Zoller, Phys. Rev. Lett. **81**, 3108 (1998).
[21] M. Greiner, O. Mandel, T. Esslinger, T. W. Hansch, and I. Bloch, Nature (London) **415**, 39 (2002).
[22] D. van Oosten, P. van der Straten, and H. T. C. Stoof, Phys. Rev. A **63**, 053601 (2001).
[23] G. Betrouni, V. Rousseau, R. T. Scalettar, M. Rigol, A. Muramatsu, P. J. H. Denteneer, and M. Troyer, Phys. Rev. Lett. **89**, 117203 (2002); V. A. Kashurnikov, N. V. Prokofev, and B. V. Svistunov, Phys. Rev. A **66**, 031601(R) (2002); S. Wessel, F. Alet, M. Troyer, and G. G. Batrouni, *ibid.* **70**, 053615 (2004).
[24] A. Osterloh, L. Amico, G. Falci, and R. Fazio, Nature (London) **416**, 608 (2002).
[25] M. J. Hartmann and M. B. Plenio, Phys. Rev. Lett. **99**, 103601 (2007).
[26] E. Demler and F. Zhou, Phys. Rev. Lett. **88**, 163001 (2002).
[27] R. D. Somma, S. Boixo, and H. Barnum, e-print arXiv:0712.1008.
[28] S. Stringari, C. R. Acad. Sci., Ser. IV Phys. Astrophys. **4**, 381 (2001).
[29] A $\pi/2$ rf pulse can evolve the atoms into an equal superposition of the two internal trappable states.
[30] A. Nayak and A. Vishwanath, DIMACS Technical Report, No. 2000-43 (unpublished); e-print arXiv:quant-ph/0010117.
[31] E. Altman, W. Hofstetter, E. Demler, and M. D. Lukin, New J.

Phys. **5**, 113 (2003).
[32] N. V. Vitanov, M. Fleischhauer, B. W. Shore, and. K. Bergmann, Adv. At., Mol., Opt. Phys. **46**, 55 (2001).
[33] K. Bergmann, H. Theuer, and B. W. Shore, Rev. Mod. Phys. **70**, 1003 (1998).
[34] K. Rodriguez, S. R. Manmana, M. Rigol, R. M. Noack, and A Muramatsu, New J. Phys. **8**, 169 (2006).
[35] P. Sengupta, M. Rigol, G. G. Batrouni, P. J. H. Denteneer, and R. T. Scalettar, Phys. Rev. Lett. **95**, 220402 (2005).
[36] Marcos Rigol and Alejandro Muramatsu, Phys. Status Solidi B **242**, 1850 (2005).
[37] L.-M. Duan, E. Demler, and M. D. Lukin, Phys. Rev. Lett. **91**, 090402 (2003); L. Santos, M. A. Baranov, J. I. Cirac, H.-U. Everts, H. Fehrmann, and M. Lewenstein, *ibid.* **93**, 030601 (2004); B. Damski, H. Fehrmann, H.-U. Everts, M. Baranov, L. Santos, and M. Lewenstein, Phys. Rev. A **72**, 053612 (2005); S. V. Isakov, S. Wessel, R. G. Melko, K. Sengupta, and Y. B. Kim, Phys. Rev. Lett. **97**, 147202 (2006); G. Grynberg, B. Lounis, P. Verkerk, J.-Y. Courtois, and C. Salomon, Phys. Rev. Lett. **70**, 2249 (1993); K. I. Petsas, A. B. Coates, and G. Grynberg, Phys. Rev. A **50**, 5173 (1994); P. Rabl, A. J. Daley, P. O. Fedichev, J. I. Cirac, and P. Zoller, Phys. Rev. Lett. **91**, 110403 (2003).
[38] V. Boyer, R. M. Godun, G. Smirne, D. Cassettari, C. M. Chandrashekar, A. B. Deb, Z. J. Laczik, and C. J. Foot, Phys. Rev. A **73**, 031402(R) (2006).
[39] O. Mandel, M. Greiner, A. Widera, T. Rom, T. W. Hansch, and I. Bloch, Phys. Rev. Lett. **91**, 010407 (2003).
[40] C. M. Chandrashekar, Phys. Rev. A **74**, 032307 (2006).
[41] Distance at which the diameter of the spot size increases by a factor of $\sqrt{2}$.